Journal of Power Sources 206 (2012) 97–102

Contents lists available at SciVerse ScienceDirect

Journal of Power Sources

journal homepage: www.elsevier.com/locate/jpowsour

The importance of water in the polyol synthesis of carbon supported platinum–tin oxide catalysts for ethanol electrooxidation

Bo Liu[a], Zhi-Wen Chia[b], Zhen-You Lee[a], Chin-Hsien Cheng[a], Jim-Yang Lee[a,*], Zhao-Lin Liu[c]

[a] Chemical & Biomolecular Engineering, National University of Singapore, 4 Engineering Drive 4, Singapore 117576, Singapore
[b] NUS Graduate School for Integrative Sciences & Engineering (NGS), Centre for Life Sciences (CeLS), #05-01 28 Medical Drive, Singapore 117456, Singapore
[c] Institute of Materials Research and Engineering, 3 Research Link, Singapore 117602, Singapore

ARTICLE INFO

Article history:
Received 23 November 2011
Received in revised form
30 December 2011
Accepted 31 December 2011
Available online 28 January 2012

Keywords:
Electrocatalyst
Ethanol electrooxidation reaction
Direct ethanol fuel cell
Polyol synthesis

ABSTRACT

Sn-modified platinum catalysts are presently one of the most active catalysts for the room temperature electrooxidation of ethanol at low potentials. In this study, Pt–SnO_x/C catalysts are prepared by the polyol method in different ethylene glycol–water mixtures using a Pt:Sn atomic ratio of 3 in the preparation solution. When the water content in the synthesis is very low (2 vol.%), only a limited amount of Sn can be incorporated into the catalyst (Pt:Sn atomic ratio of 91:9). Increasing the water content in the synthesis increases the Sn content and the intrinsic activity for ethanol electrooxidation by the "bifunctional catalysis" mechanism; however, water content in excess of 50 vol.% is counterproductive since there is a corresponding growth in the catalyst particle size which results in a reduction of the electrochemically active surface area (ECSA). Experimentally a 50:50 (vol./vol.) mixture of ethylene glycol and water is the most effective since all the precursor metals in the preparation solution can be completely transferred to the target catalyst. The advantages are not only limited to composition control (concordance of catalyst composition and solution composition in preparation), but also a small particle size (~2.2 nm) and the highest mass activity.

1. Introduction

The sluggish kinetics of the ethanol electrooxidation reaction (EOR) have been a major challenge for the direct ethanol fuel cells (DEFCs) [1–3]. Pt/C catalysts suitably modified with Sn can significantly increase the EOR activity at relative low potentials [4–6]. The good activity is generally attributed to the "bifunctional catalysis" mechanism where the Sn sites supply surface oxygen-containing species to react with the intermediates in the dissociative adsorption of ethanol on the Pt sites [7,8].

The preparation of Sn-modified Pt catalysts for EOR can be based on several approaches such as the "Bonneman" method [9], the "Pechini–Adams" method [10], and the co-reduction of metal precursors with hydrogen [11,12], formic acid [13], sodium borohydride ($NaBH_4$) [14], ethylene glycol [6,15,16] or a few others. Among them the polyol synthesis, in which ethylene glycol serves the multiple roles of solvent, reducing agent, and capping agent (after partial oxidation), has been one of the most convenient methods for producing catalytic nanoparticles in the size range of about 3 nm which are well dispersed on the catalyst support [17,18].

Neat ethylene glycol is often used as the solvent for the preparation of Pt/C and Pt–Ru/C catalysts by the polyol method [19–21]; however, when it comes to the preparation of Sn-modified Pt catalysts, water was added as a co-solvent in many of the published procedures [5,6,16], resulting in Sn existing primarily as tin oxides in the final catalysts [22]. This could be attributed to the difficulty in the reduction of Sn salts or Sn oxides by the polyol method, as indicated by Larcher et al. [23]. The importance of water in the preparation of Sn-modified Pt catalysts by the polyol method, and the quantification of the amount used, has not been systematically investigated. Indeed the difference in the amount of water used, which was not mentioned in some of these publications, could be the reason for the inconsistency in some of the reported results. For example, Jiang et al. prepared a Pt–SnO_x/C catalyst with a Pt:Sn ratio of 3:1 in the starting mixture by the polyol method and reported the catalyst composition to be 75.4:24.5 [24]. When Mann et al. repeated the same preparation procedure, the product was a catalyst with a Pt:Sn ratio of 83.5:16.5 [25]. The lack of concordance of experimental results could be due to the omission of the amount of water used in the preparation.

It is worth noting that such inconsistencies in the catalyst Pt:Sn ratio are quite common in the preparation of Sn-modified Pt catalysts by different methods [12,26]. In order to obtain an electrocatalyst with the desired Pt:Sn atomic stoichiometry, the synthesis details must be cautiously controlled [12]. To the best

* Corresponding author. Tel.: +65 65162186; fax: +65 67791936.
E-mail address: cheleejy@nus.edu.sg (J.-Y. Lee).

0378-7753/$ – see front matter © 2012 Elsevier B.V. All rights reserved.
doi:10.1016/j.jpowsour.2011.12.065

of our knowledge, there was no previous report on the control of the Pt:Sn ratio in a polyol synthesis. This study aims to quantify and understand the presence of water in the preparation of Pt–SnO_x/C catalysts by the polyol method.

2. Experimental

2.1. Synthesis of Pt–SnO_x/C electrocatalysts

$H_2PtCl_6{\cdot}6H_2O$ (99.9%, Alfa Aesar), $SnCl_2{\cdot}2H_2O$ (98%, Alfa Aesar), ethylene glycol (99%, Merck) and carbon black (Vulcan XC-72R, Cabot) were the starting materials for the synthesis of Pt–SnO_x/C catalysts. Water for preparation was 18 MΩ Millipore deionized water. In a typical preparation, 53.1 mg $H_2PtCl_6{\cdot}6H_2O$ and 7.8 mg $SnCl_2{\cdot}2H_2O$ were dissolved in 49 mL of an ethylene glycol–water mixture to form a clear solution. 1 mL 5 M NaOH aqueous solution was then introduced followed by the addition of 80 mg of carbon black. The resulting suspension was ultrasonicated for half an hour and then heated to 160 °C. It was kept at this temperature for 3 h before returning to room temperature by natural cooling. 1 M HCl was then introduced to release the Pt–SnO_x nanoparticles from the in situ formed capping agents and to deposit the nanoparticles on the carbon support. Centrifugation was then applied to recover the catalyst from the reaction mixture. After copious washing with water and ethanol thrice, the washed solid was dried in vacuum at 120 °C for 8 h and then heated in air at 200 °C for 1 h to remove remnant organic residues and to convert all Sn to Sn oxide. The catalysts prepared as such were designated as Pt–SnO_x/C (98:2), Pt–SnO_x/C (70:30), Pt–SnO_x/C (50:50) and Pt–SnO_x/C (30:70), respectively, where the numbers in the parenthesis indicate the relative volumes of ethylene glycol to water used in the preparation.

2.2. Catalyst characterizations

The catalyst metallic compositions were determined by inductively coupled plasma-mass spectrometry (ICP-MS) analysis on an Agilent 7500 ICP-MS. The overall Pt:Sn ratios were also measured by energy dispersive X-ray spectroscopy (EDX) during scanning electron microscopy (SEM) sessions on a JEOL JSM-5600LV equipped with an Oxford Instruments INCAx-act EDX analyzer. X-ray photoelectron spectroscopy (XPS) on a Kratos AXIS Hsi spectrometer using monochromatic Al Kα X-ray source was used to measure the catalyst surface Pt:Sn ratios. Powder X-ray diffraction (XRD) patterns of the catalysts were recorded by a Bruker GADDS diffractometer with an area detector, employing a Cu K_α source (λ = 1.54056 Å) operating at 40 kV and 40 mA. A JEOL JEM-2100F high-resolution transmission electron microscope (HRTEM) operating at 200 kV accelerating voltage was used to measure the metal particle size distribution.

2.3. Electrochemical measurements

All electrochemical measurements were performed on a μAutolab type III potentiostat/galvanostat using a standard three-electrode setup where the counter electrode was a Pt gauze and the reference electrode was a Ag|AgCl (in 3 M KCl) electrode. The working electrode was a glassy carbon disc (Φ5 mm) with 4 μg of Pt which was prepared as follows: 20 mg of the catalyst powder was dispersed in 10 mL of a mixture of 4.9 mL ethanol, 4.9 mL water and 0.2 mL 5% Nafion solution (Aldrich); ultrasonicated for 30 min. 10 μL of the catalyst ink prepared as such was dispensed onto the glassy carbon disk electrode and dried at room temperature. For the measurements a working electrode was first cycled in 0.1 M $HClO_4$ solution between 0 and 1.0 V at 100 mV s^{-1} for 100 cycles to clean the catalyst surface; after which a steady cyclic voltammetric response was obtained. The measurements of ethanol electrooxidation activities were carried out in a 1 M ethanol solution in 0.1 M $HClO_4$, which had been deaerated by flowing Ar before the experimental run. All the potentials in this report have been converted to the normal hydrogen electrode (NHE) scale.

3. Results and discussion

3.1. Electrocatalyst characterizations

The metal loading, overall and surface Pt:Sn atomic ratios, average particle size and electrochemically active surface area (ECSA) of the electrocatalysts prepared for this study are summarized in Table 1. Although all catalysts were prepared with the same precursor composition in the starting mixture, the actual compositions of the four Pt–SnO_x/C catalysts were different, demonstrating the effect of water content on catalyst preparation. When the water content in the preparation was very low (2 vol.%), the loadings of Pt and Sn were 19.6 wt.% and 1.18 wt.%, respectively; yielding a catalysts with a Pt:Sn atomic ratio of 91:9. The significant deviation from the Pt:Sn ratio of 3:1 in the starting mixture indicates a substantial loss of Sn during synthesis. The loss of Sn to the solution was less if water was added to ethylene glycol. For example, when ethylene glycol was mixed with 25% of water by volume, the Pt content in the catalyst was 19.5 wt.%; the Sn loading increased correspondingly to 1.93 wt.%; thus improving the Pt:Sn atomic ratio to 86:14. Complete utilization of all of the Sn in the reaction mixture was possible with a water content of 50 vol.% and beyond, and the Pt:Sn ratio in the catalysts became equal to that in the starting mixture. The catalyst surface composition as measured by XPS also changed in a corresponding manner. Fig. 1 shows the XPS spectra of the Pt–SnO_x/C catalysts in the Pt 4f and Sn 3d regions. The Sn 3d to Pt 4f peak intensity ratio increased initially from Pt–SnO_x/C (98:2) to Pt–SnO_x/C (50:50) and then leveled off somewhere between Pt–SnO_x/C (50:50) and Pt–SnO_x/C (30:70). The increasing presence of Sn in the Pt–SnO_x/C catalysts is therefore congruent with the overall composition trend measured by ICP and EDX. The Pt:Sn ratios on the surface of the Pt–SnO_x/C catalysts calculated from the XPS measurements are also provided in Table 1. Although the changes in the Sn content in both bulk and surface compositions followed the same trend, the percentage of Sn on the surface was always higher than that in the bulk for all of the catalysts. The surface enrichment by Sn oxide could be attributed to the greater affinity of Sn for oxygen than for Pt, thereby driving the migration of Sn to the surface.

Fig. 2 shows the XRD patterns of Pt–SnO_x/C catalysts prepared with different amounts of water. In addition to the peak at 2θ of about 25° from the carbon support, all catalysts exhibited the characteristic (1 1 1), (2 0 0), (2 2 0) and (3 1 1) diffractions of Pt at 2θ of 39.8°, 46.2°, 67.5° and 81.3°, respectively. There were no peak shifts to indicate the formation of Pt–Sn alloy. The non-appearance of Pt–Sn alloy could be attributed to the heat treatment of the as-synthesized catalysts in air at 200 °C for 1 h when Sn was completely oxidized to Sn oxide; same as the previous findings of Adzic et al. [5]; however, there were no detectable diffraction peaks for the Sn oxide, suggesting that the latter existed in the amorphous form.

The Pt(2 2 0) peak was used to determine the average particle size by the Debye–Scherer equation [27], and the results are shown in Table 1. An average particle size as small as 2.2 nm was obtainable when the vol.% of water was lower than 50%. The particle size increased to 3.1 nm when the water vol.% increased to 70%. The particle size and size distribution could also be measured more directly by TEM. Fig. 3a and b is typical TEM images of Pt–SnO_x/C (98:2) and Pt–SnO_x/C (70:30) catalysts, respectively, showing a good dispersion of the particles on the carbon support.

Table 1
Metal loading, Pt:Sn atomic ratios, particle sizes and electrochemically active surface area (ECSA) of the synthesized Pt–SnO_x/C catalysts.

Electrocatalyst	Metal loading (wt.%)			Pt:Sn ratio (at./at.)			Particle size (nm)		ECSA ($m^2\ g^{-1}{}_{Pt}$)
	Pt	Sn	Total	ICP	EDX	XPS	TEM	XRD	
Pt–SnO_x/C (98:2)	19.6	1.18	20.8	91:9	91:9	6.6:1	2.1	2.2	44.5
Pt–SnO_x/C (70:30)	19.5	1.93	21.4	86:14	86:14	3.3:1	2.1	2.2	43.2
Pt–SnO_x/C (50:50)	18.8	4.02	22.8	74:26	74:26	2.1:1	2.2	2.2	41.1
Pt–SnO_x/C (30:70)	19.0	4.05	23.1	74:26	74:26	2.2:1	3.0	3.1	35.5

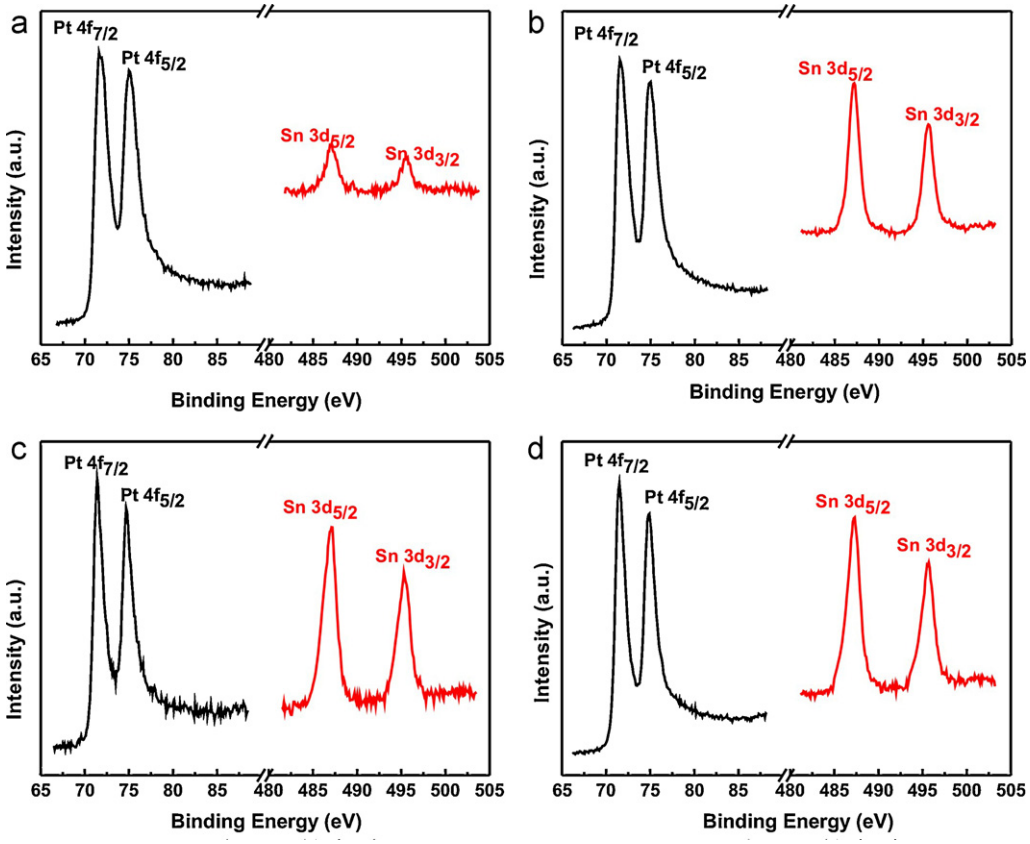

Fig. 1. Pt 4f and Sn 3d XPS spectra of (a) Pt–SnO_x/C (98:2); (b) Pt–SnO_x/C (70:30); (c) Pt–SnO_x/C (50:50); (d) Pt–SnO_x/C (30:70) electrocatalysts. The Sn 3d spectra were included in the Pt spectra without changing its intensity relative to Pt.

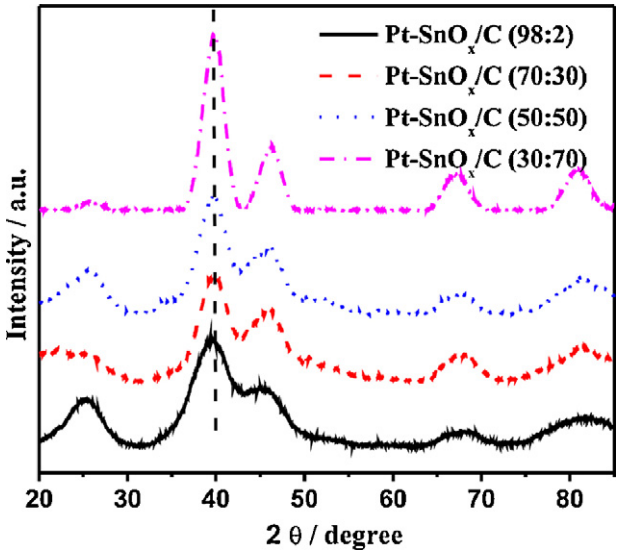

Fig. 2. XRD patterns of Pt–SnO_x/C catalysts prepared in different ethylene glycol–water mixtures.

Particle aggregation began to appear when the % water by volume was about 50%, as shown in Fig. 3c. Further increase in the water content to 70% caused severe agglomeration, which was found in the Pt–SnO_x/C (30:70) catalyst (Fig. 3d). The average particle size, determined from counting 100 nanoparticles in randomly selected regions, were 2.1 nm for Pt–SnO_x/C (98:2) and Pt–SnO_x/C (70:30), 2.2 nm for Pt–SnO_x/C (50:50) and 3.0 nm for Pt–SnO_x/C (30:70). These results, also summarized in Table 1, are in agreement with the XRD measurements.

3.2. Electrochemical measurements

Working electrodes loaded with different Pt–SnO_x/C catalysts were first cleaned by cycling between 0 and 1.0 V at 50 mV s^{-1} in 0.1 M $HClO_4$ solution until a stable voltammetric response was obtained. The stabilized cyclic voltammograms of the four Pt–SnO_x/C catalysts are shown in Fig. 4. All voltammograms contain a hydrogen adsorption/desorption region below 0.3 V, followed by a double layer charging/discharging region, and an oxide formation/reduction region. The ECSAs estimated from the hydrogen adsorption/desorption region using the corresponding value of 0.21 mC cm^{-2} are given in Table 1 [28]. Among the catalysts

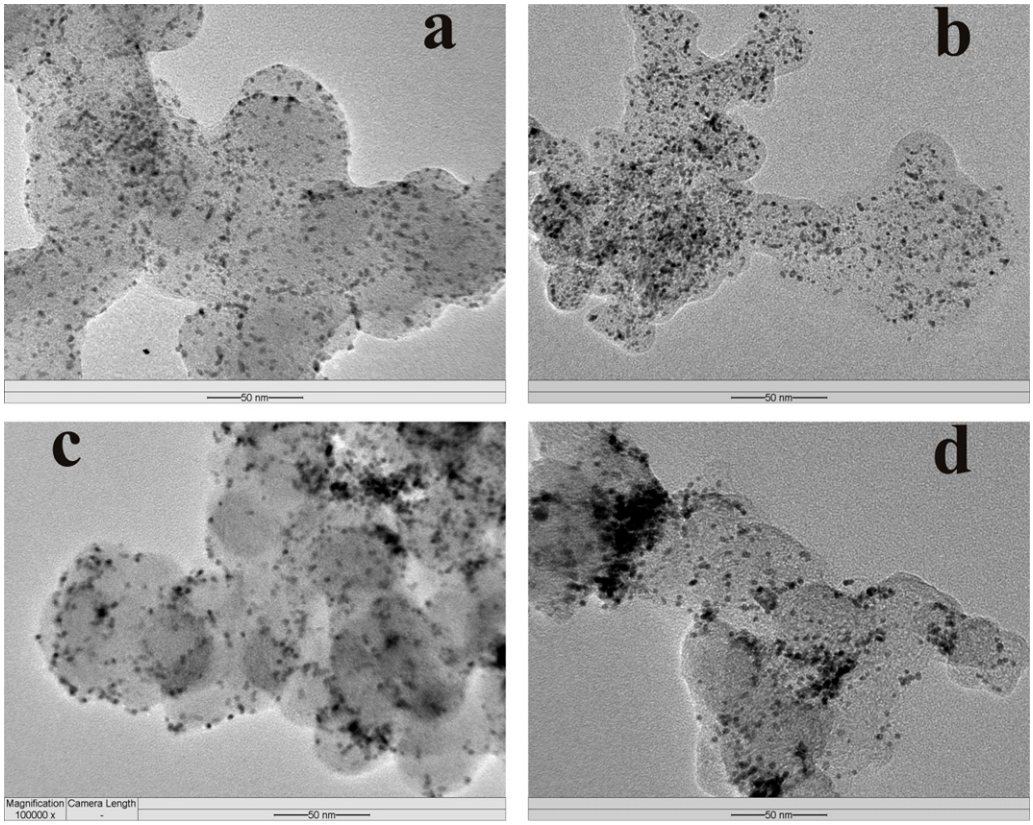

Fig. 3. Typical TEM images of Pt–SnO_x/C catalysts prepared in different glycol–water mixtures: (a) Pt–SnO_x/C (98:2); (b) Pt–SnO_x/C (70:30); (c) Pt–SnO_x/C (50:50); (d) Pt–SnO_x/C (30:70).

Pt–SnO_x/C (98:2) had the highest ECSA of 44.5 $m^2\,g^{-1}{}_{Pt}$, followed by Pt–SnO_x/C (70:30) (43.2 $m^2\,g^{-1}{}_{Pt}$) and Pt–SnO_x/C (50:50) (41.1 $m^2\,g^{-1}{}_{Pt}$). The ECSA of Pt–SnO_x/C (30:70) catalyst was the lowest at only 35.5 $m^2\,g^{-1}{}_{Pt}$. The low ECSA of Pt–SnO_x/C (30:70) was not surprising in view of its large metal particle size and observation of particle agglomeration. For the other three Pt–SnO_x/C catalysts which had similar particle size of about 2.1 nm, the ECSA decreased gradually with the increase in Sn content, which could be explained by the coverage of some Pt surface atoms by Sn oxide.

The EOR activities of the catalysts were measured by cyclic voltammetry in 1 M ethanol in 0.1 M $HClO_4$ at a scan rate of 5 mV s^{-1}. The anodic scan currents in the voltammograms normalized by the mass of Pt are shown in Fig. 5. Among the catalysts Pt–SnO_x/C (98:2) showed the least EOR mass activity. The EOR mass activity increased progressively with the water content in preparation up to 50 vol.%, indicating the beneficial effect of a relative increase in the Sn content of the catalysts made possible by the increasing presence of water in the polyol synthesis; however, when the water content in the reaction medium was greater than 50 vol.%, the EOR mass activity decreased due to the compensation

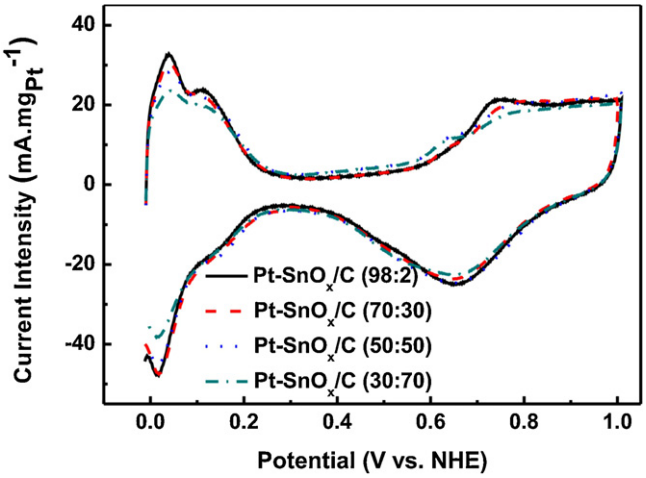

Fig. 4. Cyclic voltammograms of different Pt–SnO_x/C catalysts in 0.1 M $HClO_4$ at a scan rate of 50 mV s^{-1}. All experiments were performed at room temperature.

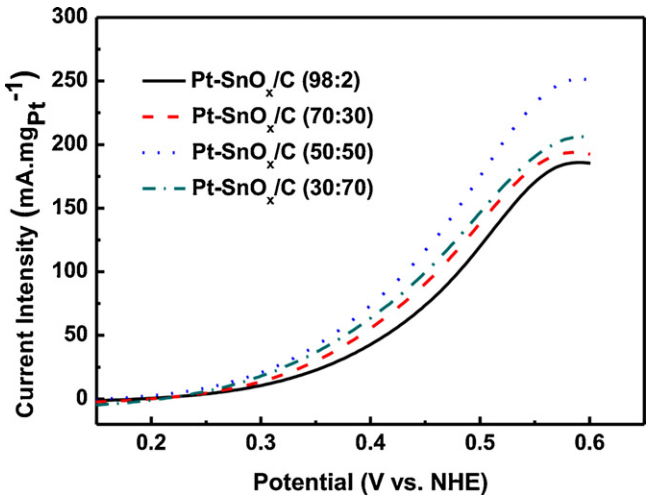

Fig. 5. Anodic sweep cyclic voltammograms of different Pt–SnO_x/C catalysts in 1 M ethanol solution in 0.1 M $HClO_4$ at a scan rate of 5 mV s^{-1}. All experiments were performed at room temperature.

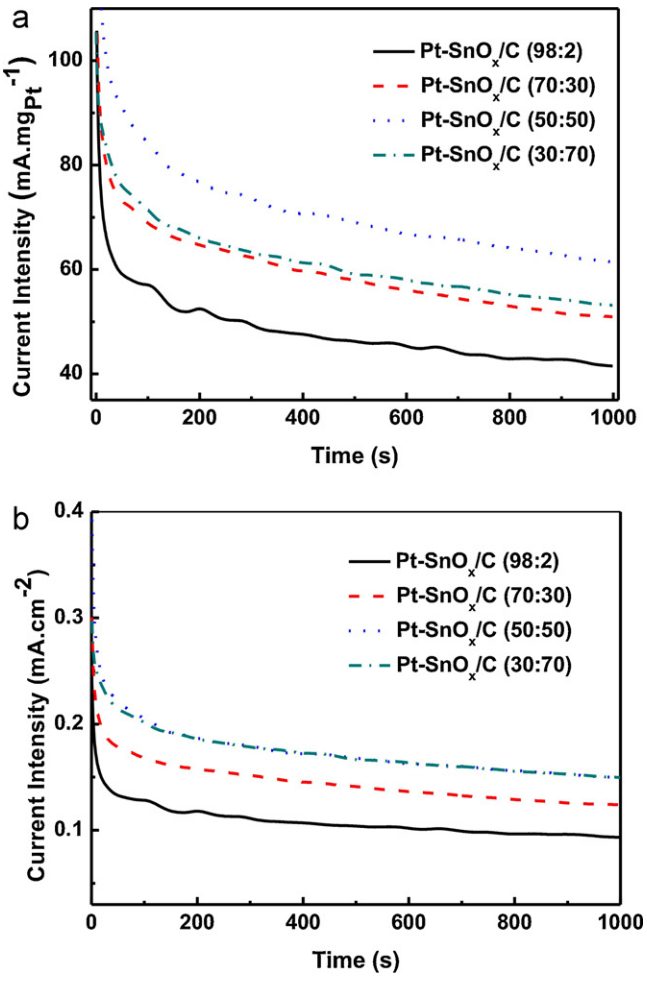

Fig. 6. Chronoamperograms of electrooxidation of 1 M ethanol in 0.1 M $HClO_4$ on the polyol-synthesized Pt–SnO_x/C catalysts at 0.45 V: (a) current density normalized by the Pt mass (mass activity) and (b) current density normalized by the ECSA (specific activity). All experiments were performed at room temperature.

effect from an increase in the particle size, and hence a decrease in the ECSA.

The EOR activities of the polyol-synthesized Pt–SnO_x/C catalysts were also evaluated by chronoamperometry (CA) in 1 M ethanol in 0.1 M $HClO_4$ at 0.45 V. This particular potential was chosen because it is close to the anode working potential in actual direct ethanol fuel cells. Fig. 6a shows the activity on Pt mass basis as a function of time. The EOR activities of all catalysts decreased sharply in the first 60 s, indicating the rapid buildup of intermediates from the dissociative chemisorption of ethanol. The EOR mass activity of Pt–SnO_x/C (50:50) at 1000 s was 61.4 mA $mg^{-1}{}_{Pt}$, the highest among the catalysts. The next was Pt–SnO_x/C (30:70) (53.2 mA $mg^{-1}{}_{Pt}$ at 1000 s) followed by Pt–SnO_x/C (70:30) (51.2 mA $mg^{-1}{}_{Pt}$ at 1000 s). Pt–SnO_x/C (98:2) with a mass activity of only 41.7 mA $mg^{-1}{}_{Pt}$ at 1000 s, was the least active electrocatalyst for EOR. There is therefore congruence between the chronoamperometric and voltammetric results. Specific activity, which is measured as current divided by ECSA, is generally regarded as a measure of the electrocatalyst intrinsic activity because the definition factors out the first order effect of the surface area. The specific activities of the EOR catalysts were therefore calculated and re-plotted in Fig. 6b. In this different basis of representation the Pt–SnO_x/C (30:70) catalyst behaved nearly identically as Pt–SnO_x/C (50:50) (overlapping CA curves and a specific activity of 0.15 mA cm^{-2} at 1000 s). The specific activities of Pt–SnO_x/C (70:30) and Pt–SnO_x/C (98:2) were lower, at 0.12 mA cm^{-2} for the former and 0.094 mA cm^{-2} for the latter at 1000 s. It is therefore apparent that the intrinsic activity for EOR increased with the increase in the Sn content in the synthesized Pt–SnO_x/C catalysts.

Sn, either in the alloy form with Pt or as an oxide in the vicinity of Pt nanoparticles, has been an effective promoter for the Pt catalysts in EOR; allowing the oxidation of ethanol to occur at low potentials. A few studies have attempted to compare the relative contributions of Pt–Sn alloy and Sn oxide in EOR, however, no conclusion could be drawn because of inconsistent results. For example, the promotional effect of Sn oxide to Pt–Sn alloy for EOR was reported by Jiang et al. [29] and by Sen Gupta et al. [30]. On the contrary, Colmenares et al. [31] and Godoi et al. [32] found greater enhancements of the EOR activity in catalysts with more Pt–Sn alloy than Sn oxide. More interestingly, Colmati et al. suggested that Sn oxide enhances the EOR activity at low temperature and/or at low current densities, whereas alloyed Sn is more effective for EOR at high temperature and/or at high current densities [13]. Zhu et al. observed similar results and further suggested that Sn oxide facilitates the production of acetic acid; whereas Pt–Sn alloy promote the formation of acetaldehyde [33]. Compared with the possible multiple roles of Sn in a Pt–Sn alloy for EOR (e.g. electronic effects that cause weaker ethanol adsorption; and the increase in the lattice parameter that facilitates C—C bond cleavage); the promotional effect of Sn oxide is relatively simple and may be attributed to mostly the "bifunctional catalysis" mechanism, where Sn oxide is capable of water activation at potentials lower than that is required for Pt [4,5,30]. The OH groups formed are effective for the removal of dehydrogenated products from the dissociative adsorption of ethanol on Pt [7,8]. Thus, the intrinsic activity of Pt benefited from and increased with the presence of Sn oxide; as long as the latter are in close proximity of the Pt sites. Hence Pt–SnO_x/C (98:2), which had the largest ECSA among all catalysts, was ineffective due to the absence of Sn oxide. When the water content in the polyol reaction was lower than 50 vol.%, the Sn content increased with the water content without much changes in the ECSA; hence intrinsic activity increased in the order of Pt–SnO_x/C (98:2) < Pt–SnO_x/C (70:30) < Pt–SnO_x/C (50:50). A water content higher than 50 vol.% in the polyol synthesis did not change the Sn content. Instead, there was a more substantial decrease in the ECSA due to increased particle aggregation. The benefit of Sn oxide addition was therefore negated by a smaller ECSA. Hence even though Pt–SnO_x/C (30:70) and Pt–SnO_x/C (50:50) had the same intrinsic activities, the Pt–SnO_x/C (30:70) catalyst was poorer in mass activity.

4. Conclusions

Pt–SnO_x/C catalysts are prepared by the polyol method in ethylene glycol–water mixtures with a starting Pt:Sn atomic ratio of 3 but different water contents. The water content in the preparation is found to play an important role. On one hand, the addition of water increases the Sn content in the Pt–SnO_x/C catalysts due to a more complete utilization of Sn in the reaction mixture, which gives rise to higher EOR activities which are normalized by the catalyst ECSA. On the other hand, more water also increases particle growth and particle agglomeration, which results in low ECSAs and hence reduces the Pt utilization. The most optimal reaction medium for the preparation of Pt–SnO_x/C catalyst with a Pt:Sn atomic ratio of 3 is a mixture with equal volumes of ethylene glycol and water: not only can all of the Sn be recovered with Pt from the solution, but it also yields a catalyst with the highest mass and specific activities for EOR.

Acknowledgement

This research is financially supported by research grant R279-000-272-112 from the Ministry of Education, Singapore.

References

[1] J.P.I. de Souza, S.L. Queiroz, K. Bergamaski, E.R. Gonzalez, F.C. Nart, J. Phys. Chem. B 106 (2002) 9825–9830.
[2] N. Tian, Z.-Y. Zhou, S.-G. Sun, Y. Ding, Z.L. Wang, Science 316 (2007) 732–735.
[3] H.-F. Wang, Z.-P. Liu, J. Am. Chem. Soc. 130 (2008) 10996–11004.
[4] A. Kowal, M. Li, M. Shao, K. Sasaki, M.B. Vukmirovic, J. Zhang, N.S. Marinkovic, P. Liu, A.I. Frenkel, R.R. Adzic, Nat. Mater. 8 (2009) 325–330.
[5] M. Li, A. Kowal, K. Sasaki, N. Marinkovic, D. Su, E. Korach, P. Liu, R.R. Adzic, Electrochim. Acta 55 (2010) 4331–4338.
[6] W. Zhou, Z. Zhou, S. Song, W. Li, G. Sun, P. Tsiakaras, Q. Xin, Appl. Catal. B 46 (2003) 273–285.
[7] A.V. Tripkovic, K.D. Popovic, J.D. Lovic, V.M. Jovanovic, S.I. Stevanovic, D.V. Tripkovic, A. Kowal, Electrochem. Commun. 11 (2009) 1030–1033.
[8] S. Garcia-Rodriguez, F. Somodi, I. Borbath, J.L. Margitfalvi, M.A. Pena, J.L.G. Fierro, S. Rojas, Appl. Catal. B 91 (2009) 83–91.
[9] C. Lamy, S. Rousseau, E.M. Belgsir, C. Coutanceau, J.M. Léger, Electrochim. Acta 49 (2004) 3901–3908.
[10] F.L.S. Purgato, P. Olivi, J.M. Léger, A.R. de Andrade, G. Tremiliosi-Filho, E.R. Gonzalez, C. Lamy, K.B. Kokoh, J. Electroanal. Chem. 628 (2009) 81–89.
[11] F. Vigier, C. Coutanceau, A. Perrard, E.M. Belgsir, C. Lamy, J. Appl. Electrochem. 34 (2004) 439–446.
[12] S. García-Rodríguez, M.A. Peña, J.L.G. Fierro, S. Rojas, J. Power Sources 195 (2010) 5564–5572.
[13] F. Colmati, E. Antolini, E.R. Gonalez, J. Electrochem. Soc. 154 (2007) B39–B47.
[14] J.H. Kim, S.M. Choi, S.H. Nam, M.H. Seo, S.H. Choi, W.B. Kim, Appl. Catal. B 82 (2008) 89–102.
[15] P.E. Tsiakaras, J. Power Sources 171 (2007) 107–112.
[16] E.V. Spinacé, M. Linardi, A.O. Neto, Electrochem. Commun. 7 (2005) 365–369.
[17] W. Yu, W. Tu, H. Liu, Langmuir 15 (1998) 6–9.
[18] C. Bock, C. Paquet, M. Couillard, G.A. Botton, B.R. MacDougall, J. Am. Chem. Soc. 126 (2004) 8028–8037.
[19] Q. Wang, G.Q. Sun, L.H. Jiang, Q. Xin, S.G. Sun, Y.X. Jiang, S.P. Chen, Z. Jusys, R.J. Behm, Phys. Chem. Chem. Phys. 9 (2007) 2686–2696.
[20] J. Ye, J. Liu, Z. Zou, J. Gu, T. Yu, J. Power Sources 195 (2010) 2633–2637.
[21] Z.L. Liu, L. Hong, M.P. Tham, T.H. Lim, H.X. Jiang, J. Power Sources 161 (2006) 831–835.
[22] L. Jiang, G. Sun, Z. Zhou, S. Sun, Q. Wang, S. Yan, H. Li, J. Tian, J. Guo, B. Zhou, Q. Xin, J. Phys. Chem. B 109 (2005) 8774–8778.
[23] D. Larcher, R. Patrice, J. Solid State Chem. 154 (2000) 405–411.
[24] L.H. Jiang, G.Q. Sun, S.G. Sun, J.G. Liu, S.H. Tang, H.Q. Li, B. Zhou, Q. Xin, Electrochim. Acta 50 (2005) 5384–5389.
[25] J. Mann, N. Yao, A.B. Bocarsly, Langmuir 22 (2006) 10432–10436.
[26] D.L. Boxall, E.A. Kenik, C.M. Lukehart, Chem. Mater. 14 (2002) 1715–1720.
[27] V. Radmilovic, H.A. Gasteiger, P.N. Ross, J. Catal. 154 (1995) 98–106.
[28] J. Zhao, P. Wang, W.X. Chen, R. Liu, X. Li, Q.L. Nie, J. Power Sources 160 (2006) 563–569.
[29] L. Jiang, Z. Zhou, W. Li, W. Zhou, S. Song, H. Li, G. Sun, Q. Xin, Energy Fuels 18 (2004) 866–871.
[30] S. Sen Gupta, S. Singh, J. Datta, Mater. Chem. Phys. 116 (2009) 223–228.
[31] L. Colmenares, H. Wang, Z. Jusys, L. Jiang, S. Yan, G.Q. Sun, R.J. Behm, Electrochim. Acta 52 (2006) 221–233.
[32] D.R.M. Godoi, J. Perez, H.M. Villullas, J. Power Sources 195 (2010) 3394–3401.
[33] M.Y. Zhu, G.Q. Sun, Q. Xin, Electrochim. Acta 54 (2009) 1511–1518.